

Ionization of Interstellar Hydrogen Beyond the Termination Shock

Mike Gruntman

Department of Astronautical Engineering, University of Southern California,
Los Angeles, CA 90089-1192

mikeg@usc.edu

Abstract. Models of solar wind interaction with the surrounding interstellar medium usually disregard ionization of interstellar hydrogen atoms beyond the solar wind termination shock. If and when included, the effects of ionization in the heliospheric interface region are often obscured by complexities of the interaction. This work assesses the importance of interstellar hydrogen ionization in the heliosheath. Photoionization could be accounted for in a straightforward way. In contrast, electron impact ionization is largely unknown because of poorly understood energy transfer to electrons at the termination shock and beyond. We first estimate the effect of photoionization and then use it as a yardstick to assess the role of electron impact ionization. The physical estimates show that ionization of interstellar hydrogen may lead to significant mass loading in the inner heliosheath which would slow down plasma flowing toward the heliotail and deplete populations of nonthermal protons, with the corresponding effect on heliospheric fluxes of energetic neutral atoms.

1. Introduction

The supersonic solar wind plasma undergoes a shock transition at large heliocentric distances and fills the region between the termination shock and the heliopause, the inner heliosheath. (In the article, the word heliosheath is used in the sense of the inner heliosheath.) There, the plasma flows into the heliospheric tail where it eventually mixes with the surrounding local interstellar medium (LISM). Charge exchange of energetic protons on interstellar hydrogen atoms in the heliosheath produces heliospheric energetic neutral atom (ENA) fluxes (e.g., [1] and references therein).

Two Voyager spacecraft crossed the termination shock at 94 AU and 84 AU from the Sun in 2004 and 2007, respectively, and entered the heliosheath (e.g., [2,3,4,5,6]). In 2009, the Interstellar Boundary Explorer (IBEX) mission obtained the first maps of the heliospheric interface in ENA fluxes [7] which revealed many details of the global solar wind interaction with the surrounding LISM. Cassini spacecraft also imaged the heliosphere in ENA fluxes at somewhat higher energies of atoms [8]. In-situ measurements by Voyagers and remote observations by IBEX and Cassini found a number of unexpected phenomena at the interstellar boundary of the solar system (e.g., [9]). In particular, definitive explanation of a discovered by IBEX unanticipated standing-out band of enhanced ENA emissions across the sky, the ribbon [7,10], remains challenging. A recent review [30] lists multiple possible competing concepts of this phenomena. Failure of predicting and difficulties in reproducing the ribbon in simulations of heliospheric interactions suggest that some important physical phenomena may not be identified yet and/or properly included into models.

Understanding properties of the shocked solar wind plasma between the termination shock and heliopause is indispensable for explaining observed heliospheric ENA fluxes. Even most sophisticated global models introduce important simplifications. Most common assumptions include multi-fluid and



magneto-hydrodynamic descriptions of flows of gases and plasmas and Maxwellian or other postulated velocity distributions of plasma protons. Such physical simplifications and assumptions lead to uncertainties in comparing results of model simulations with observations which are hard to quantify and they are rarely, if ever, pointed out and discussed in publications.

Available Voyager in-situ measurements of the bulk solar wind plasma and higher energy (>20 keV) protons [2,4,5] incompletely characterize the termination shock. Downstream of the shock, the heliosheath plasma is not in equilibrium, with nonthermal protons accounting for most energy density while most mass and inertia being in relatively cold protons [8,10,11]. The plasma properties may not even be stationary due to solar cycle variations of the global solar wind properties. Coulomb collisions are so rare in the heliosheath, even among electrons, that they could usually be disregarded.

The complexity of the solar wind interaction with the LISM obscures and makes it difficult to assess relative importance of particular physical processes. For example, many otherwise sophisticated and complex models of the interaction disregard, without sound justification, solar photoionization and electron impact ionization in the heliosheath [9]. Photoionization is often considered to be negligible while electron impact ionization tacitly assumed either inconsequential or too complex and uncertain for inclusion into models.

Recent physical estimates show that ionization of interstellar atomic hydrogen in the heliosheath could significantly modify plasma flow patterns beyond the termination shock and heliospheric ENA fluxes [9]. This work explores effects of ionization on the plasma properties in the heliosheath. Investigation of particular contributions of other physical processes such as charge exchange is outside the scope of the article.

2. Solar photoionization

At large distances from the Sun both solar photoionization and the neutral component of the solar wind disturb the partially ionized interstellar gas, the interstellar wind, approaching the solar system. The effect of photoionization on the LISM beyond the heliopause is relatively small. In contrast, the neutral solar wind flux could significantly change the interstellar wind properties ([9], [12] and references therein).

Absorption of the solar extreme ultraviolet radiation on the heliospheric scales is negligible, and the photoionization rate of hydrogen atoms is thus inversely proportional to the square of the heliocentric distance. One can calculate the photoionization rate from solar radiation spectra.

Consider, for example, interstellar hydrogen atoms approaching the solar system with the velocity 25 km s^{-1} . A small fraction, about 0.5%, of interstellar atoms would be photoionized when they reach the heliocentric distance 130 AU under moderate solar conditions [9]. For a LISM with neutral hydrogen atoms twice more abundant than protons, photoionization would increase interstellar plasma effective temperature (by adding energetic photoelectrons) by about 100 K.

Clearly, solar photoionization is not particularly important for modifying properties of interstellar gas entering the heliosheath. However, even its small photoionization could produce a significant effect on the rarefied heliosheath plasma because the latter is two orders of magnitude less dense than interstellar neutrals. The heliosheath plasma flow picks up photoionization-produced protons and electrons, resulting in its mass loading. Electron impact ionization of atoms also adds to mass loading. While one can include photoionization into modeling in a straightforward way, accounting for electron impact ionization presents major difficulties.

To estimate the effect of photoionization, let us consider a typical simplified axisymmetric heliospheric interaction [13] shown in figure 1 (left) and calculated for realistic parameters of the LISM and the solar wind. For the upwind (interstellar wind) direction, the distances to the termination shock, heliopause, and bow shock are 89 AU, 152 AU, and 270 AU, respectively. The polar angle θ is counted from the upwind direction, and the angle-dependent heliocentric distances to the termination shock and heliopause are $R_{\text{TS}}(\theta)$ and $R_{\text{HP}}(\theta)$, respectively. The heliosheath plasma (gray region in the figure) flows across (not necessarily normally) a side surface of a cone with the half-angle θ between heliocentric distances $R_{\text{TS}}(\theta)$ and $R_{\text{HP}}(\theta)$. All the solar wind flow that crosses the termination shock at angles $< \theta$ would be evacuated to the heliospheric tail through this side surface of the cone.

Consider the isotropic supersonic solar wind consisting of only protons and electrons with the constant velocity and the flux number density inversely proportional to the square of the heliocentric distance. Let us assume that at the distance $R_0 = 1$ AU from the Sun the solar wind flux density is $f_0 = 2.2 \times 10^8 \text{ cm}^{-2} \text{ s}^{-1}$; the solar photoionization rate is $\beta_{s,0} = 1.0 \times 10^{-7} \text{ s}^{-1}$ (moderate solar activity); and that the LISM atomic hydrogen uniformly fills space with the number density $n_0 = 0.18 \text{ cm}^{-3}$.

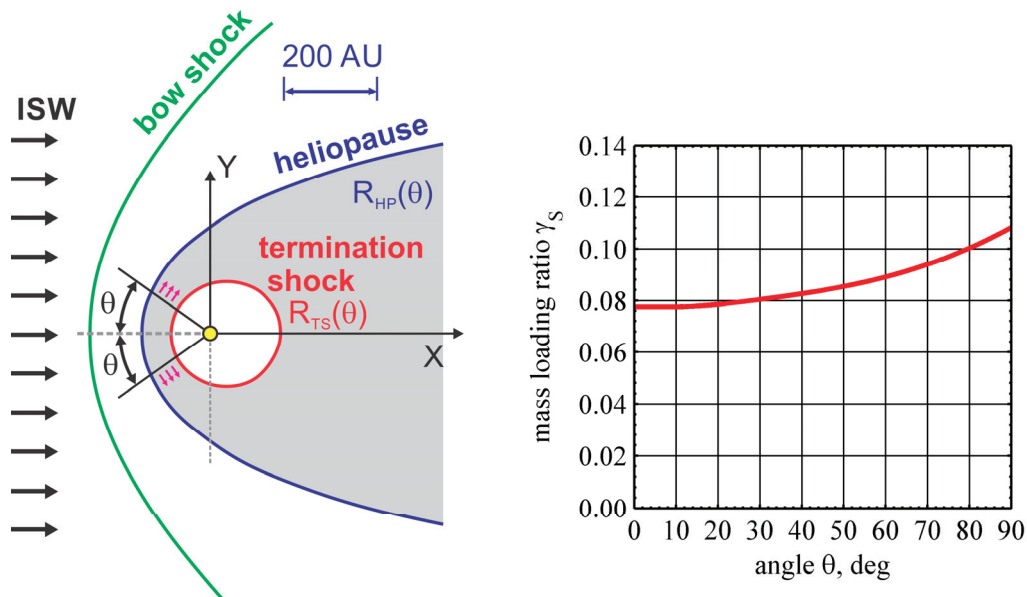


Figure 1. Left: schematic of a typical simplified axisymmetric heliospheric interaction with the bow shock, heliopause, and termination shock calculated in [13]. The angle θ is counted from the upwind (interstellar wind) direction. Small arrows show the heliosheath plasma (gray area) flow across the side surface of a cone with a half-angle θ . Right: angular dependence of the mass loading coefficient $\gamma_s(\theta)$ due to photoionization.

One can define the mass loading coefficient (ratio) of the plasma flow, $\gamma_s(\theta) = \alpha_s(\theta)/\Phi(\theta)$, as the ratio of the additional photoionization-produced plasma mass flow $\alpha_s(\theta)$ to the solar wind mass flow $\Phi(\theta)$ across a side cone surface of the heliosheath region restricted by the half-angle θ . Then,

$$\gamma_s(\theta) = g_0 \frac{\Gamma(\theta)}{1 - \cos \theta},$$

where one independent of the interaction geometry dimensionless coefficient,

$$g_0 = \frac{n_0 \beta_{s,0} R_0}{f_0},$$

describes solar and interstellar conditions while the other dimensionless parameter,

$$\Gamma(\theta) = \frac{1}{R_0} \int_0^\theta [R_{\text{HP}}(\theta) - R_{\text{TS}}(\theta)] \sin \theta d\theta,$$

characterizes the geometric properties of the heliosheath [9].

Figure 1 (right) shows the angular dependence of the mass loading coefficient $\gamma_s(\theta)$ that increases from $\gamma_s = 0.078$ at small angles θ to $\gamma_s = 0.108$ at $\theta = 90^\circ$. So, photoionization of interstellar atomic hydrogen would increase the heliosheath plasma mass flow by approximately one tenth when it reaches

and crosses the annulus at $\theta = 90^\circ$. The mass loading coefficient increases to 0.15 and 0.18 in the heliospheric tail at distances of 200 AU and 300 AU, respectively [9]. So, photoionization would increase the mass flow of the solar wind by roughly one-fifths in the distant heliotail. For the purposes of this work, exact parameters of the interstellar medium and the solar wind are not particularly important as we focus on nonstrictly self-consistent physical estimates of ionization effects for a typical geometry.

3. Electron impact ionization

First attempts to account for electron impact ionization of interstellar hydrogen atoms beyond the termination shock in global heliospheric models date back to mid-1990s [14]. The process remains often disregarded to this date which is sometimes explained by complexity of its inclusion into models (e.g., [15]). When this ionization is accounted for, models usually assume Maxwellian distributions of electrons at plasma temperatures [13,16,17,18].

The energy-dependent cross-section of electron impact ionization of hydrogen atoms peaks in the 30–130 eV energy range. Let us assume the uniform electron (and proton) number density $n_e = 10^{-3} \text{ cm}^{-3}$ in the heliosheath, consistent with the Voyager 2 observations [19]. One can calculate the electron impact ionization rate $\beta_e(T_e)$ of atoms by averaging over electron velocities. Figure 2 shows the temperature dependence of the rate $\beta_e(T_e)$ for electrons with a Maxwellian velocity distribution function at temperature T_e and negligible velocity of interstellar hydrogen atoms; two horizontal lines at $1.0 \times 10^{-11} \text{ s}^{-1}$ and $0.44 \times 10^{-11} \text{ s}^{-1}$ are the photoionization rates of atomic hydrogen at distances 100 AU and 150 AU from the Sun, respectively.

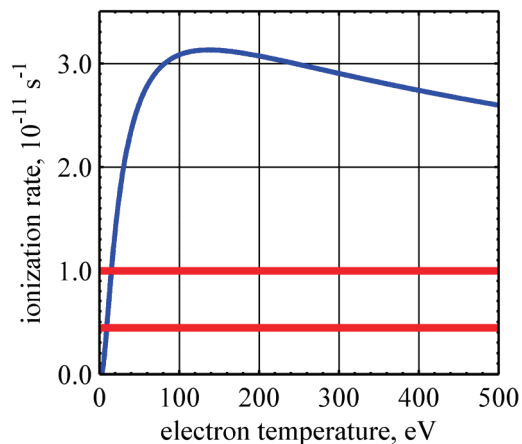


Figure 2. Temperature dependence of the ionization rate (blue curve) of hydrogen atoms in the heliosheath by electrons with a Maxwellian distribution and number density $n_e = 10^{-3} \text{ cm}^{-3}$.

Two solid horizontal straight red lines correspond to the photoionization rates (moderate solar activity) $1.0 \times 10^{-11} \text{ s}^{-1}$ and $0.44 \times 10^{-11} \text{ s}^{-1}$ of interstellar hydrogen atoms at representative for the inner heliosheath distances 100 AU and 150 AU from the sun, respectively.

One can see that electron impact ionization may be significantly higher than photoionization in the heliosheath. At the same time the properties of electrons in this region remain unknown. The originally formulated concept of heliosphere ENA imaging that led to the IBEX mission had specifically pointed out lack of knowledge of “how the solar wind energy is redistributed between the proton and electron components of the postshock plasma” [20] downstream of the termination shock. There is no definitive and validated by measurements answer to this question yet, which is fundamentally important for understanding ionization in the heliosheath.

The only existing in-situ plasma measurements in the heliosheath did not probe properties of electrons in detail. One Faraday cup (side sensor D) of the Voyager 2 plasma instrument is sensitive to electrons with 10–5950 eV energies. Electron fluxes are too low, however, for reliable measurements in the distant solar wind and in the heliosheath (Richardson, 2015, private communications). Moreover, it is unclear how exactly absence of measurable electron fluxes constrains effective electron temperatures that could possibly range, as discussed below, from a few eV up to a few hundred eV. Therefore, electron

impact ionization could be significantly larger than photoionization everywhere in the heliosheath, with an important effect on the plasma flow especially if electron temperatures exceed 20–30 eV.

Ionization of interstellar hydrogen increases the number density of the heliosheath plasma. It also changes effective electron temperatures in the region. Consequently, local electron impact ionization rates also change as they depend on both the number density and temperature. The average energy of photoelectrons produced by photoionization under moderate solar activity conditions is approximately 4.2 eV. Injection of such electrons into the heliosheath plasma would heat or cool its electron component depending on whether the initial temperature is lower than a few eV or higher than several eV, respectively. In addition, each act of electron impact ionization "removes" the hydrogen atom ionization energy, 13.6 eV, from the electron population. If one assumes instantaneous accommodation and Maxwellization of electrons, then ionization would increase electron temperatures in one year by 10% and 20% for the heliosheath plasma with initial electron temperatures 45 eV and 92 eV, respectively [9]. Note that it takes several years for the solar wind plasma to convect through the heliosheath and reach the distant heliotail. Consequently, if the initial effective electron temperature is $T_e > 50$ eV, then the already dominating electron impact ionization rate may increase substantially, for example double, in a control volume of the heliosheath plasma as it flows to the tail. Such an increase would be especially pronounced if initial electron temperatures are 100 eV or higher.

The concept of heating or cooling of the bulk plasma electrons is applicable only if photoelectrons reach a local equilibrium with a Maxwellian velocity distribution. Such Maxwellization not necessarily happens in the plasma of the heliosheath where Coulomb collisions are rare and negligible. (In contrast, the electron-electron collision mean free path is about 1 AU beyond the heliopause in the LISM.) So, it is not excluded that ionization-created electrons preserve their energies to some extent. Then, photoionization, for example, could produce a population of electrons with energies 0–50 eV in the heliosheath plasma, with abundances ~10% in sidewind directions at $\theta = 90^\circ$ and ~20% in the heliotail.

4. Discussion

Photoionization alone could mass-load plasma flows by 10-20% in the heliosheath. The magnitude of this effect in some areas near the heliopause where the plasma flow slows down would be significantly larger. Figure 2 shows that electron impact ionization could be much more efficient than photoionization. At the same time, the former process is entirely ignored in the models because very little is known about electron velocity distributions in the heliosheath.

The plasma instrument on Voyager 2 directly measured velocities of the bulk solar wind plasma across the termination shock and in the heliosheath [5,19,21]. About 200 days before the termination shock crossing, the solar wind velocity was 380 km s^{-1} which corresponded to proton kinetic energy 750 eV. The flow then slowed down to about 310 km s^{-1} , or 500 eV per proton, immediately upstream of the termination shock. Downstream of the shock, the velocity dropped to 120 km s^{-1} and the corresponding 80-eV energy per proton. Voyager 2 also observed increase of the proton temperature across the shock to 10^5 K , with the corresponding average energy of proton thermal motion 13 eV.

So, about 650 eV energy per each original solar wind (not pickup) proton is transferred in the shock transition to the nonthermal proton population, solar wind electrons, plasma waves, and acceleration of higher energy ions. How exactly this transferred, or "lost," energy is partitioned among these possibilities is an important key to understanding the heliospheric interaction. For higher solar wind velocities characteristic for ecliptic polar regions during solar minima, the lost energy may be as large as 2 keV per solar wind proton, significantly larger than the conditions encountered by Voyager 2.

Observed by IBEX heliospheric ENA fluxes in the 0.5-6.0 keV energy range [10] do not seem to require transfer of energy from the bulk solar wind protons to ENA-producing nonthermal proton populations [9]. The abundance of the latter is also consistent with that of the pickup protons in the solar wind upstream of the termination shock. The energy balance then suggests that the measured 650-eV energy loss by each solar wind proton is transferred to electrons and to protons with energies $> 6 \text{ keV}$ in the termination shock transition.

Therefore, one arrives at two contrasting possibilities based on energy conservation in the shock transition, one with the negligibly small and the other with the non-negligible fractions of the bulk solar

wind energy imparted to electrons in the heliosheath. In the former case, effective electron temperature would be only a few eV or smaller with the resulting electron impact ionization of interstellar hydrogen smaller than photoionization. In the latter case, electron impact ionization dominates and it could be an order of magnitude higher than photoionization if electron temperatures are 50 eV or higher (figure 2). Electron impact ionization becomes prominent in the heliosheath if only a small fraction, just one-twentieth or one-tenth of the energy lost by the bulk solar wind plasma upstream of the termination shock, is transferred to electrons. Even as much transferred energy as 100 eV or 200 eV per electron would not contradict current interpretations of experimental results or theoretical considerations regarding acceleration of higher energy particles at and beyond the termination shock.

The plasma instrument on Voyager 2 seems to be the only source of possible in-situ observational constraints on electron temperatures in the heliosheath. However, it has not detected any electron signal [5]. The situation is further complicated as the heliosheath plasma is essentially not Coulomb collisional and electron energy distributions could thus deviate from Maxwellian. Interplanetary shocks, for example, produce copious populations of 30-150 eV electrons [22]. It was recently suggested that higher energy electrons in the heliosheath may charge the Voyager spacecraft [23]. As a result, such an effect may lead to a significant increase of the possible upper limit on electron temperatures implied by absence of the measured electron signal.

Very few publications tried to theoretically consider properties of electrons in the termination shock transition and beyond. They all pointed to fundamental unresolved difficulties in understanding and describing such processes [23,24,25,26]. It was also noted that higher electron temperatures could lead to significant thermal conductivity in the heliosheath which would further modify the structure of the heliospheric interface [26].

The effect of interstellar hydrogen ionization is essentially nonlinear as the resulting mass loading slows down the plasma flow, causes compression, and further increases importance of continuing ionization. In addition, the heliosheath plasma continuously emits ENAs and thus loses its momentum and energy. The rate of electron impact ionization also increases as electrons are added to the slowing heliosheath plasma. As a result, one could expect a significant ionization effect on the heliosheath plasma in the upwind hemisphere. The distant heliospheric tail is another region where accumulated mass loading would strongly modify plasma flow properties and ENA emissions.

It is possible that temporal solar-cycle variations of the global solar wind might create conditions where a plasma flow could come practically to rest at some regions of the heliosheath, especially in the upwind direction near the heliopause. For example, unexplained properties of the so called "knot" in IBEX ENA images [10,27,30] may be a manifestation of such a phenomenon driven in part by ionization. A volume of plasma with near-zero flow velocities could first produce enhanced ENA emissions as it piles up and becomes denser and then its intensity decreases as the nonthermal proton population is depleted, the latter process sometimes described as plasma "aging" [9].

For example, a population of protons with 3-keV energy would decrease by a factor of 50 in 7 years and ENA fluxes produced by such protons practically vanish [9]. Note that a volume of plasma with typical flow velocities 150 km s^{-1} , as those observed by Voyager 2 in the heliosheath [19], would move by 220 AU in 7 years which is about the characteristic size of the heliosphere. Therefore, the solar wind plasma initially flowing into the upwind hemisphere contributes very little to ENA fluxes at such energies when it reaches the heliospheric tail at distances of 150 AU from the sun and beyond.

Depletion of ENA-producing proton populations is highly sensitive to slowing down of the plasma flow in the heliosheath and thus strongly depends on mass loading and, in turn, on the ionization rate of interstellar hydrogen. For example, just a one-year increase of the effective age of protons, from 4 to 5 years, at 3 keV would decrease ENA intensities at this energy by a factor of 2 [9]. Mass loading due to photoionization alone could produce such an effect in parts of the heliosheath. The existing observations and conservation of energy do not seem to preclude transfer of a fraction of bulk solar wind energy to the heliosheath electrons and hence causing efficient electron impact ionization that could alter plasma flows even to a greater extent. Therefore, inclusion of interstellar hydrogen ionization into heliospheric models and computer simulations is indispensable for understanding the heliosheath. Disregarding this effect could make comparison of model predictions with the in-situ and ENA observations difficult and uncertain.

Global heliospheric models are already highly complex which obscures relative importance of various physical processes involved. Dedicated parametric studies of the effects of ionization on observable ENA fluxes could advance understanding of the interaction. Present descriptions of the heliospheric interaction almost exclusively rely on the Euler variables for flow fields. Following evolution of plasma parameters in the Lagrange variables for control mass along flow lines could provide important insight to the heliosheath plasma and determine contributions of various physical processes to ENA intensity maps.

Advancing theoretical understanding of energy transfer to electrons in the termination shock transition is essential for accurate accounting of ionization of interstellar hydrogen and its effect on the heliosheath plasma. No reliable in-situ measurements of electrons at the termination shock and in the heliosheath exist or are expected in the foreseeable future. Therefore, in the near term, it is important to quantitatively determine how absence of measured electron fluxes by the Voyager 2 plasma instrument beyond the termination shock constrains possible effective temperatures and velocity distributions of electrons. In the longer term, in-situ measurement of electron properties should be among top priorities for the future Interstellar Probe mission [28, 29 and references therein].

Acknowledgments

This work is supported, in part, by NASA's IBEX program.

5. References

- [1] Gruntman M 1997 Imaging of space plasmas in energetic neutral atom fluxes *Rev. Sci. Instrum.* **68** 3617–56
- [2] Decker R B, Krimigis S M, Roelof E C, Hill M E, Armstrong T P, Gloeckler G, Hamilton D C, and Lanzerotti L J 2005 Voyager 1 in the foreshock, termination shock, and heliosheath *Science* **309** 2020–24
- [3] Stone E C, Cummings A C, McDonald F B, Heikkila B C, Lal N, and Webber W R 2005 Voyager 1 explores the termination shock region and the heliosheath beyond *Science* **309** 2017–20
- [4] Decker R B, Krimigis S M, Roelof E C, Hill M E, Armstrong T P, Gloeckler G, Hamilton D C, and Lanzerotti L J 2008 Mediation of the solar wind termination shock by non-thermal ions *Nature* **454** 67–70
- [5] Richardson J D, Kasper J C, Wang C, Belcher J W, and Lazarus A J 2008 Cool heliosheath plasma and deceleration of the upstream solar wind at the termination shock *Nature* **454** 71–74
- [6] Stone E C, Cummings A C, McDonald F B, Heikkila B C, Lal N, and Webber W R 2008 An asymmetric solar wind termination shock *Nature* **454** 71–74
- [7] McComas D J et al 2009 First global observations of the interstellar interaction from the Interstellar Boundary Explorer *Science* **326**, 959–62
- [8] Krimigis S M, Mitchell D G, Roelof E C, Hsieh K C, and McComas D J 2009 Imaging the interaction of the heliosphere with the interstellar medium from Saturn with Cassini *Science* **326** 971–3
- [9] Gruntman M 2015 Interstellar hydrogen ionization in the heliosheath *J. Geophys. Res.* **120** 6119–32
- [10] Funsten H O et al 2009 Structures and spectral variations of the outer heliosphere in IBEX energetic neutral atom maps *Science* **326** 964–6
- [11] Roelof E C, Krimigis S M, Mitchell D G, Decker R B, Richardson J D, Gruntman M, and Funsten H O 2010 Implications of generalized Rankine-Hugoniot conditions for the PUI population at the Voyager 2 termination shock *Proc. 9th Ann. Intern. Astrophys. Conf., AIP Conf. Proc.* **1302** 133–41
- [12] Gruntman M 1982 Effect of neutral component of solar wind on the interaction of the Solar system with the interstellar gas flow *Sov. Astron. Lett.* **8**(1) 24–6
- [13] Izmodenov V, Malama Y G, Gloeckler G, and Geiss J 2003 Effects of interstellar and solar wind ionized helium on the interaction of the solar wind with the local interstellar medium *Astroph. J. Lett.* **594** L59–62

- [14] Baranov V B and Malama Y G 1996 Axisymmetric self-consistent model of the solar wind interaction with the LISM: basic results and possible ways of development *Space Sci. Rev.* **78** 305–16
- [15] Alouani-Bibi F, Opher M, Alexashov D, Izmodenov V, and Toth G 2011 Kinetic versus multi-fluid approach for interstellar neutrals in the heliosphere: exploration of the interstellar magnetic field effects *Astrophys. J.* **734** 45
- [16] Izmodenov V V and Baranov V B 2006 Modern multi-component models of the heliospheric interface *The Physics of the Heliospheric Boundaries, V. Izmodenov and R. Kallenbach (eds.), ESA-ESTEC, Paris ISSI Scientific Report No. 5* 67–135
- [17] Malama Y G, Izmodenov V V and Chalov S V 2006 Modeling of the heliospheric interface: multi-component nature of the heliospheric plasma *Astron. Astrophys.* **445** 693–701
- [18] Scherer K, Fichtner H, Fahr H-J, Bzowski M, and Ferreira S E S 2014 Ionization rates in the heliosheath and in astrosheaths: spatial dependence and dynamical relevance *Astron. Astrophys.* **563** A69
- [19] Richardson J D and Decker R B 2015 Plasma and flows in the heliosheath *J. Phys.: Conf. Ser.*, **577** 012021
- [20] Gruntman M, Roelof E C, Mitchell D G, Fahr H J, Funsten H O, and McComas D J 2001 Energetic neutral atom imaging of the heliospheric boundary region *J. Geophys. Res.* **106** 15767–81
- [21] Richardson J D and Wang C 2012 Voyager 2 observes a large density increase in the heliosheath *Astrophys. J. Lett.* **759** L19
- [22] Isenberg P.A. and Feldman W C 1997 Electron-impact ionization of interstellar hydrogen and helium at interplanetary shocks *Geophys. Res. Lett.* **22** 873–5
- [23] Fahr H J, Richardson J D, and Verscharen D 2015 The electron distribution function downstream of the solar-wind termination shock: Where are the hot electrons? *Astron. Astrophys.* **579** A18
- [24] Chalov S V and Fahr H J 2013 The role of solar wind electrons at the solar wind termination shock *Month. Not. Roy. Astron. Soc.* **433** L40–3
- [25] Chashei I V and Fahr H J 2013 On the electron temperature downstream of the solar wind termination shock *Ann. Geophys.* **31** 1205–12
- [26] Izmodenov V V, Alexashov D B, and Ruderman M S 2014 Electron thermal conduction as a possible physical mechanism to make the inner heliosphere thinner *Astrophys. J. Lett.* **795** L7
- [27] McComas D J. et al. 2010 Evolving outer heliosphere: large-scale stability and time variations observed by the Interstellar Boundary Explorer *J. Geophys. Res.* **115** A09113
- [28] Gruntman M 2004 Instrumentation for interstellar exploration *Adv. Space Res.* **34(1)** 204–12
- [29] McNutt Jr. R L, Gruntman M, Krimigis S M, Roelof E C, Wimmer-Schweingruber R F 2011 Interstellar Probe: Impact of the Voyager and IBEX results on science and strategy *Acta Astronautica* **69** 767–76
- [30] McComas D.J, Lewis W S, and Schwadron N.A. 2014 IBEX's Enigmatic Ribbon in the sky and its many possible sources *Rev. Geophys.* **52** 118-155